2012

Size and phase control of cobalt-carbide nanoparticles using OH- and Cl- anions in a polyol process

Zachary J. Huba
Virginia Commonwealth University

Everett E. Carpenter
Virginia Commonwealth University, ecarpenter2@vcu.edu

Huba, Z. J., and Carpenter, E. Size and phase control of cobalt-carbide nanoparticles using OH- and Cl- anions in a polyol process. Journal of Applied Physics, 111, 07B529 (2012).

Size and phase control of cobalt–carbide nanoparticles using OH^- and Cl^- anions in a polyol process

Zachary J. Huba and Everett E. Carpenter[a)]
Department of Chemistry, Virginia Commonwealth University, Richmond, Virginia 23284, USA

(Presented 2 November 2011; received 23 September 2011; accepted 21 November 2011; published online 8 March 2012)

Exchange coupled cobalt–carbide nanocomposites and single-phase Co_2C nanoparticles were synthesized using the polyol process. Hydroxide and chloride anions were used to control carbide phase and particle shape. Synthesized Co_xC nanocomposites exhibited average diameters around 300 nm. Co_xC nanocomposites synthesized at 0.25 M $[OH^-]$ and $[Cl^-]$ formed clusters of capped nanorods, whereas synthesis at 0.37 M $[OH^-]$ and $[Cl^-]$ produced clusters of long blade-like particles. For single-phase Co_2C, an $[OH^-]$ and $[Cl^-]$ of 0.71 M was used and produced clusters of ellipsoidal grains. The Co_xC nanocomposites comprised of capped nanorods possessed a BH_{max} of 1.65 MGOe with a magnetic saturation and coercivity values of 38 emu/g and 2.4 kOe, respectively. Co_2C possessed a saturation magnetization of 16 emu/g and coercivity of 1.3 kOe. © *2012 American Institute of Physics*. [doi:10.1063/1.3677816]

I. INTRODUCTION

Industrial permanent-magnet applications are dominated by rare-earth-based materials.[1,2] However, with the substantial energy products intrinsic to rare-earth-based permanent magnets also comes substantial cost. Non-rare-earth-based permanent magnets are attractive because of their lower cost of starting materials, but possess significantly lower energy products when compared to their rare-earth counterparts.[1] Hence, the development of new non-rare-earth-based permanent magnets is of emerging interest.

Through the use of a wet chemical processing technique, the synthesis of permanent-magnetic cobalt–carbide (Co_xC) nanoparticles represents one of the few recent developments in permanent-magnet materials. Co_xC nanoparticles are commonly synthesized as nanocomposites of the Co_2C and Co_3C phases.[3,4] The reconstruction caused by the doping of carbon into the metallic cobalt structure increases the magnetocrystalline anisotropy, and is a cause for the observed coercivity. The Co_xC nanoparticles are synthesized using the polyol process. The polyol process has been used extensively in the past to synthesize metal and oxide nanoparticles, whereby a metal salt is dissolved in a polyhydric alcohol (polyol) and heated to elevated temperatures. The polyol acts as a solvent, and a reducing and capping agent.

Whereas early reports have shown Co_xC particles to possess permanent-magnet properties, further optimization of magnetic properties is required for Co_xC particles to compete with other permanent-magnetic materials.[3] Control of shape and Co_xC phase composition are two possible ways to enhance the energy product of Co_xC particles. Surfactants are commonly used for shape control in the polyol process.[4,5] For metallic cobalt particles synthesized using the polyol process, $[OH^-]$ has been shown to both affect shape and metallic cobalt phase.[6–10] The chloride anion can also be used to control size and shape by oxidatively etching the particle surface and preventing polycrystalline agglomeration.[11,12] In this paper, various $[OH^-]$ and $[Cl^-]$ are used to synthesize Co_xC nanocomposite particles and single-phase Co_2C. By investigating the affects of shape and phase on magnetic properties, further optimization of Co_xC nanoparticles could lead to new high-energy product non-rare-earth permanent magnets.

II. EXPERIMENTAL

To synthesize Co_xC particles, 0.50 g (0.002 mol) of cobalt acetate tetrahydrate and appropriate amounts of KOH and KCl were added to 50 mL of tetraethylene glycol in a round bottom flask. The OH^-:Cl^- ratio was maintained at 1 for each synthesis. The contents of the flask were then heated to 295 °C under distillation conditions and mechanical stirring for 15 min. The solution was then cooled for 1 h to room temperature. Particles were magnetically separated from the supernatant and rinsed with methanol numerous times. The collected particles were then dried in a vacuum oven at room temperature.

Crystal-phase identification of the particles was carried out on an MPD X-Ray Diffractometer (XRD) utilizing a Pixcel detector. Crystal-phase composition was determined using X'Pert HighScore Plus software. Transmission electron micrographs (TEM) were collected using a Zeiss Libra 120 with an accelerating voltage of 120 KeV. Magnetic characterization was performed on a Quantum Design VersaLab Vibrating Sample Magnetometer. Honda-Owen plots were constructed by plotting the magnetic susceptibility against the inverse field from 20 kOe to 30 kOe. A best fit line was then calculated with the y intercept equaling the amount of paramagnetic susceptibility. Isothermal remanance magnetization (IRM) and direct current demagnetization (DCD) plots were collected as a function of applied field. For an IRM plot, the magnetization was measured at zero field, then ramped to ΔH, and returned to zero field. The magnetization

a)Electronic mail: ecarpenter2@vcu.edu.

was then measured and repeated for increasing steps of ΔH. For the DCD plots, the sample was first saturated in a negative field and returned to zero field. The magnetization was then measured as was explained for the IRM plot. ΔH for both IRM and DCD plots was 20 Oe. Henkel plots were then constructed from the IRM and DCD values using the equation: $\delta M = M_{DCD} - (1 - 2M_{IRM})$.[13]

III. RESULTS AND DISCUSSION

To control the phase composition of Co_xC particles, the rate of reduction was controlled by varying the [OH^-]. Using OH^- deprotonates the polyol creating a cobalt glycolate complex. At elevated temperatures the Co^{2+} is reduced to Co^0 and the glycol forms an ethoxy acetaldehyde.[14] We propose that the carbide formation then ocurs via a two-step process. The acetaldehyde moiety is decarbonylated by the cobalt.[15] This results in a cobalt bound to a formyl group similar to the proposed transition state during Fischer Tropsch synthesis.[16] The formyl group is then catalytically decomposed leaving carbons atoms adsorbed to the surface of the cobalt particles. The surface carbon atoms then facilitate a surface reconstruction, forming the carbide structure.[17–19] Hence, by controlling the rate of reduction with [OH^-], the amount of ethoxy acetaldehyde and the resulting surface carbon atoms can be controlled. To allow for complete reconstruction, polycrystalline agglomeration of the cobalt particles must be attenuated. The effect of the Cl^- to oxidatively etch the surface of polyol synthesized particles has been commented on in the past, and is used in this study to slow the formation of polycrystalline assemblies of metallic cobalt.[11]

XRD scans of as synthesized Co_xC nanocomposites and pure phase Co_2C are shown in Fig. 1. Co_xC nanocomposites were synthesized at [OH^-] and [Cl^-] concentrations of 0.25 M and 0.37 M. The percent phase compositions (Co_3C:Co_2C) for particles synthesized at 0.25 M and 0.37 M were 60:40 and 70:30, respectively. Single-phase Co_2C was formed using a 0.71 M [OH^-] and [Cl^-] solution. Along with altering crystal phase, [OH^-] and [Cl^-] can also affect the morphology of particles.[6–11]

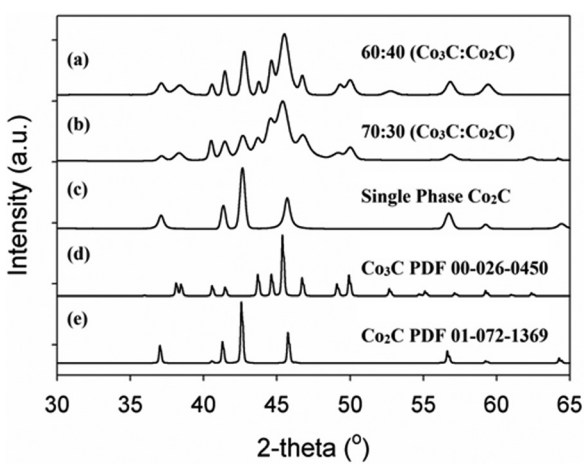

FIG. 1. XRD scans of as synthesized Co_xC particles at [OH^-] and [Cl^-] of (a) 0.25 M, (b) 0.37 M, and (c) 0.71 M, with (d) Co_3C reference pattern (PDF 00-026-0450), and (e) Co_2C reference pattern (PDF 01-072-1369) shown at the bottom.

TEM images of as synthesized Co_xC are shown in Figs. 2(a)–2(e). Particles synthesized using a 0.25 M [OH^-] and [Cl^-] in TEG solution had a diameter of 300 nm and resembled a nanoflower-like morphology with small capped rod-like assemblies on the particles edge (Fig. 2(a)). The capped nanorods ranged from 30 to 80 nm in length with an average diameter of 7 nm (Fig. 2(b)). For particles synthesized at a 0.37 M [OH^-] and [Cl^-] in TEG solution, longer acicular like projections composed the particle surface. Average particle diameter was similar to the particles synthesized at 0.25 M, but possessed a sea-urchin-like morphology (Figs. 2(c) and 2(d)). The blade-like surface protrusions measured up to 150 nm in length, as shown in Fig. 2(e). Synthesized Co_2C formed assemblies of ellipsoids and were very irregular in shape (Fig. 2(f)). The ellipsoids had diameters as large as 30 nm.

To analyze the permanent-magnetic properties for the Co_xC and Co_2C particles, magnetic moment versus applied field ($M(H)$) curves were measured at room temperature (Fig. 3). The maximum energy product (BH_{max}) was observed for the Co_xC particles with flower-like morphology at 1.65 MGOe. These particles possessed a saturation magnetization (M_s) of 38 emu/g and coercivity (H_c) of 2.4 kOe. The Co_xC particles with sea-urchin-like morphology had a similar M_s but a decrease in H_c to 1.3 kOe was observed.

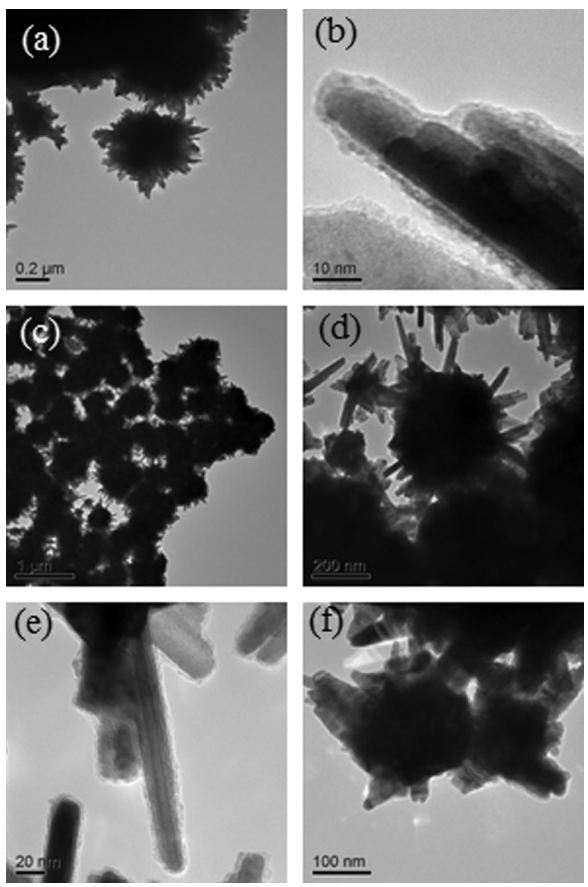

FIG. 2. TEM images of (a) flower-like Co_xC nanocomposites, and (b) nanorods comprising particle's surface, (c,d) sea-urchin-like Co_xC nanocomposites, (e) their acicular-like projections, and (f) Co_2C particles.

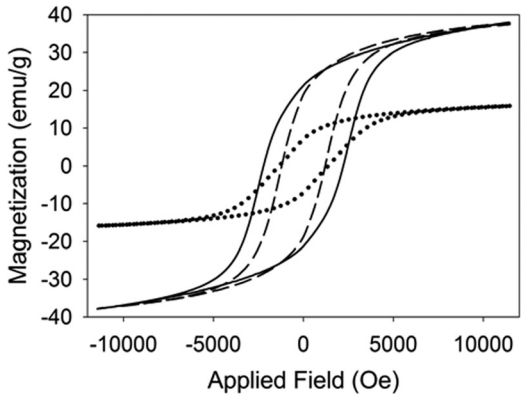

FIG. 3. Room-temperature $M(H)$ curves for flower-like (solid) and sea-urchin-like (dashed) Co_xC nanocomposites, and Co_2C (dotted) particles.

Inspection of the $M(H)$ curves for the Co_xC nanocomposites reveals that the demagnetization curve for flower-like particles have more paramagnetic character than the particles with sea-urchin-like morphology at high fields. A Honda-Owens plot revealed the flower-like particles possessed 19.07% paramagnetic character at saturation, whereas the sea-urchin-like particles had only 9.08% at saturation. The synthesized Co_2C particles showed an M_s and H_c of 16 emu/g and 1.3 kOe, respectively. The magnetizations recorded are consistent with previous reports showing Co_3C to have a higher magnetization than Co_2C.[3,4]

To investigate the magnetic interactions present in the exchange coupled cobalt–carbide nanocomposites, Henkel plots were constructed from IRM and DCD plots. For the flower-like Co_xC nanocomposites and Co_2C particles, very little magnetic domain interaction was present. However, for the Co_xC nanocomposites with sea-urchin-like morphology, demagnetizing magnetostatic interactions were present at low reversal fields, and could be one cause for the low coercivity observed. The difference in grain shape observed in each Co_xC system could also affect coercivity. Theoretical studies have shown that high-aspect-ratio rods with rounded edges possess higher shape anisotropy than rods with sharp edges and could account for the difference in coercivity observed.[20] Hence, by effectively controlling the shape of the particles, magnetostatic interactions can be eliminated and shape anisotropy can be increased, resulting in higher-energy product permanent magnets.

IV. CONCLUSION

A wet chemical technique known as the polyol process was used to synthesize permanent-magnetic Co_xC nanoparticles. Particles synthesized at 0.25 M and 0.37 M $[OH^-]$ and $[Cl^-]$ produced Co_xC nanocomposites. Single-phase Co_2C particles were synthesized at a $[OH^-]$ and $[Cl^-]$ of 0.71 M. TEM images showed the nanocomposites synthesized at 0.25 M to have a nanoflower-like morphology, with capped nanorod projections on the particle surface. Synthesis at 0.37 M $[OH^-]$ and $[Cl^-]$ produced particles with long blade-like projections, resembling a sea-urchin-like morphology. Both the flower-like, and sea-urchin-like Co_xC particles had an average particle diameter around 300 nm. Co_2C particles formed agglomerations of ellipsoidal grains. A maximum energy product of 1.65 MGOe was recorded for the Co_xC nanocomposites, with an M_s of 38 emu/g and H_c of 2.4 kOe. Co_2C particles had an M_s and H_c of 16 emu/g and 1.3 kOe, respectively. With the increased understanding of ways to control phase and shape of Co_xC particles being presented, progress can be made toward increasing the energy product of Co_xC permanent magnets.

ACKNOWLEDGMENTS

Z.J.H. and E.E.C. acknowledge the help of the Virginia Commonwealth Nanomaterials Core Characterization Facility. Z.J.H. thanks A.C.H. for help with the proofreading and revisions. This work has been funded by ARPAe.

[1]O. Gutfleisch, M. A. Willard, E. Bruck, C. H. Chen, S. G. Sankar, and J. P. Liu, Adv. Mater. **23**, 821 (2011).
[2]S. Sugimoto, J. Phys. D: Appl. Phys. **44**, 1 (2011).
[3]V. G. Harris, Y. Chen, A. Yang, S. Yoon, Z. Chen, A. L. Geiler, J. Gao, C. N. Chinnasamy, L. H. Lewis, C. Vittoria, E. E. Carpenter, K. J. Carroll, R. Goswami, M. A. Willard, L. Kurihara, M. Gjoka, and O. Kalogirou, J. Phys. D: Appl. Phys. **43**, 2656 (2010).
[4]Y. Zhang, G. S. Chaubey, C. Rong, Y. Ding, N. Poudyal, P.-C. Tsai, Q. Zhang, and J. P. Liu, J. Magn. Magn. Mater. **323**, 1495 (2011).
[5]S. I. Cha, C. B. Mo, K. T. Kim, and S. H. Hong, J. Mater. Res. **20**, 2148 (2005).
[6]N. Chakroune, G. Viau, C. Ricolleau, F. Fievet-Vincent, and F. Fievet, J. Mater. Chem. **13**, 312 (2003).
[7]T. Hinotsu, B. Jeyadevan, C. N. Chinnasamy, K. Shinoda, and K. Tohji, J. Appl. Phys. **95**, 7477 (2004).
[8]C. Osorio-Cantillo and O. Perales-Perez, J. Appl. Phys. **105**, 3 (2009).
[9]Y. Soumare, C. Garcia, T. Maurer, G. Chaboussant, F. Ott, F. Fievet, J. Y. Piquemal, and G. Viau, Adv. Funct. Mater. **19**, 1971 (2009).
[10]G. Viau, C. Garcia, T. Maurer, G. Chaboussant, F. Ott, Y. Soumare, and J. Y. Piquemal, Phys. Status Solidi A **206**, 663 (2009).
[11]B. Wiley, T. Herricks, Y. G. Sun, and Y. N. Xia, Nano Lett. **4**, 2057 (2004).
[12]J. An, B. Tang, X. L. Zheng, J. Zhou, F. X. Dong, S. P. Xu, Y. Wang, B. Zhao, and W. Q. Xu, J. Phys. Chem. C **112**, 15176 (2008).
[13]E. P. Wohlfarth, J. Appl. Phys. **29**, 595 (1958).
[14]K. J. Carroll, J. U. Reveles, M. D. Shultz, S. N. Khanna, and E. E. Carpenter, J. Phys. Chem. C **115**, 2656 (2011).
[15]T. Morimoto, K. Fuji, K. Tsutsumi, and K. Kakiuchi, Angew. Chem., Int. Ed. **42**, 2409 (2003).
[16]S. Shetty and R. A. van Santen, Catal. Today **171**, 168 (2011).
[17]J. Cheng, P. Hu, P. Ellis, S. French, G. Kelly, and C. M. Lok, J. Phys. Chem. C **114**, 1085 (2010).
[18]S. Stolbov, S. Y. Hong, A. Kara, and T. S. Rahman, Phys. Rev. B **72**, 155423 (2005).
[19]K. F. Tan, J. Xu, J. Chang, A. Borgna, and M. Saeys, J. Catal. **274**, 121 (2010).
[20]F. Ott, T. Maurer, G. Chaboussant, Y. Soumare, J. Y. Piquemal, and G. Viau, J. Appl. Phys. **105**, 013915 (2009).